Available online at www.sciencedirect.com
SCIENCE DIRECT®
Chemical Physics Letters 401 (2005) 385–392
CHEMICAL PHYSICS LETTERS
www.elsevier.com/locate/cplett

# Coupled cluster calculations of the optical rotation of *S*-propylene oxide in gas phase and solution

Jacob Kongsted [a,*], Thomas Bondo Pedersen [b], Mikkel Strange [a], Anders Osted [a], Aage E. Hansen [a,1], Kurt V. Mikkelsen [a], Filip Pawlowski [c], Poul Jørgensen [c], Christof Hättig [d]

[a] *Department of Chemistry, H. C. Ørsted Institute, University of Copenhagen, DK-2100 Copenhagen Ø, Denmark*
[b] *Department of Theoretical Chemistry, Chemical Center, University of Lund, P.O. Box 124, S-221 00 Lund, Sweden*
[c] *Department of Chemistry, University of Aarhus, Langelandsgade 140, DK-8000 Aarhus C, Denmark*
[d] *Institute of Nanotechnology, Forschungszentrum Karlsruhe, P.O. Box 3640, D-76021 Karlsruhe, Germany*

Received 28 September 2004; in final form 15 November 2004
Available online 8 December 2004

**Abstract**

We present ab initio calculations of the optical rotation of *S*-propylene oxide in both gas phase and solution using the coupled cluster methodology combined with a dielectric continuum description of the solvent. The coupled cluster calculations are performed using the CCS, CC2, CCSD and CC3 methods. None of the presented gas phase results are in accord with the experimental sign of the optical rotation at 355 nm. Thereby, the experimental sign change between the gas phase and the cyclohexane solution optical rotation at 355 nm is not reproduced theoretically. The vibrational effects are considered to be significant and may be of crucial importance in order to bring accordance between the calculated and the experimentally established sign of the gas phase optical rotation at 355 nm.
© 2004 Elsevier B.V. All rights reserved.

## 1. Introduction

In units of deg [dm g/cm$^3$]$^{-1}$, the specific optical rotation (OR) of a sample of chiral molecules is defined as

$$[\alpha]_{\tilde{\nu}} = 28800\pi^2 N_A a_0^4 \frac{\tilde{\nu}^2 \beta'(\omega)}{M}, \quad (1)$$

where $N_A$ is Avogadro's number, $a_0$ is the bohr radius in cm, $\tilde{\nu}$ is the frequency in cm$^{-1}$, $M$ is the molecular weight in g/mol, and $\beta'(\omega)$ (in atomic units, $a_0^4$) is defined in terms of the trace of the frequency-dependent electric dipole–magnetic dipole polarizability according to

$$\beta'(\omega) = -\mathrm{Im}\frac{\mathrm{Tr}\langle\langle \boldsymbol{\mu}, \mathbf{m}\rangle\rangle_\omega}{3\omega}. \quad (2)$$

The vector $\boldsymbol{\mu}$ ($\mathbf{m}$) is the electric (magnetic) dipole operator. The expression for $\beta'(\omega)$ in Eq. (2) is derived using the common length gauge (LG). However, this expression may be transformed to the (equivalent) velocity gauge expression. For exact theory the two expressions would yield identical results, whereas approximate theories generally are gauge-dependent. Here, it is sufficient to state that the coupled cluster (CC) results for the length and velocity gauge specific rotations only are

* Corresponding author. Fax: +45 35 32 02 59.
*E-mail addresses:* kongsted@theory.ki.ku.dk (J. Kongsted), Thomas.Pedersen@teokem.lu.se (T.B. Pedersen), s971493@student.dtu.dk (M. Strange), osted@theory.ki.ku.dk (A. Osted), aage@gene.ki.ku.dk (Aa.E. Hansen), kmi@theory.ki.ku.dk (K.V. Mikkelsen), filip@chem.au.dk (F. Pawlowski), pou@chem.au.dk (P. Jørgensen), christof.haettig@int.fzk.de (C. Hättig).
[1] Permanent address: Holmebjerg 5, Trørød DK-2950 Vedbæk, Denmark.

0009-2614/$ - see front matter © 2004 Elsevier B.V. All rights reserved.
doi:10.1016/j.cplett.2004.11.082

equivalent in case of an untruncated cluster operator combined with a complete basis set [1]. As a consequence, the LG results suffer from origin-dependence [2]. That is, for a translation of the origin along **a** ($\mathbf{r} \rightarrow \mathbf{r}-\mathbf{a}$), the LG specific rotation transforms as $[\alpha]_{\tilde{\nu}} \rightarrow [\alpha]_{\tilde{\nu}} + \mathbf{a}\cdot\mathbf{\Lambda}$, where the origin-dependence vector $\mathbf{\Lambda}$ is proportional to the response function $\langle\langle \mathbf{r},\mathbf{p}\rangle\rangle_{\omega}$ and where **r** (**p**) is the electronic position (momentum) operator, see e.g. [2,3] for further details. As discussed in [2], the origin-dependence may be removed without recourse to London orbitals (LAOs, or gauge including atomic orbitals, GIAOs) by using the modified velocity gauge (MVG) formulation. The latter approach consists of subtracting from the conventional velocity gauge expression the static limit, i.e. $\beta'(\omega)$ is calculated as

$$\beta'(\omega) = \mathrm{Re}\frac{\left(\mathrm{Tr}\langle\langle \mathbf{p},\mathbf{m}\rangle\rangle_{\omega} - \mathrm{Tr}\langle\langle \mathbf{p},\mathbf{m}\rangle\rangle_{0}\right)}{3\omega^2}. \tag{3}$$

For details we refer to [2]. In this Letter, we shall employ both the LG and MVG expressions for optical rotation.

Amos [4] was the first to implement an ab initio theory of optical rotatory dispersion (ORD). With the purpose of avoiding the sum over excited states, Amos used the approximation

$$\beta'(\omega) \approx \beta'(0) = -\lim_{\omega\rightarrow 0}\left(\mathrm{Im}\frac{\mathrm{Tr}\langle\langle \boldsymbol{\mu},\mathbf{m}\rangle\rangle_{\omega}}{3\omega}\right), \tag{4}$$

which can be computed from static wave function derivatives. Using the static limit approach for the calculation of $\beta'$ combined with Eq. (1), an approximate expression for the specific rotation is obtained, where the entire frequency-dependence resides in the $\tilde{\nu}^2$ factor. Clearly, the applicability of the static approach is limited to transparent regions near zero frequency. Thus, for calculations of the specific rotation at the sodium D-line (589.3 nm), the static approach usually produces results in fairly good agreement with the full dynamical one (i.e. relying on the dynamical response function method), whereas at shorter wave lengths the results obtained by these two schemes must diverge [5]. This reflects the rather general rule that since the optical rotation must vanish at zero frequency, experimental results at longer wave lengths are easier to reproduce, at least qualitatively, than those at shorter wave lengths.

In recent years, there has been an increasing amount of theoretical work focused on the prediction of optical rotation, see e.g. [2,3,6–16]. One of the favorite molecules in these studies has been propylene oxide (also known as methyl oxirane) [2,6,7,10–16]. There are two reasons for this. First, propylene oxide is sufficiently small to allow for application of highly sophisticated ab initio or density functional theory (DFT) models in conjunction with fairly large basis sets. Second, experimental optical rotations have been measured in a range of solvents [17,18] and in the pure liquid state [17,19] as well as in gas phase [18]. In particular, Müller et al. [18] reported the first measurement of the specific rotation of *S*-propylene oxide at 355 nm to $10.2 \pm 2.9$ deg [dm g/cm$^3$]$^{-1}$ in gas phase and $-26.4$ deg [dm g/cm$^3$]$^{-1}$ in cyclohexane solution. In the pure liquid state at 16 °C, the specific rotation at the sodium D-line was reported to be $-12.53$ [dm g/cm$^3$]$^{-1}$ in [17], while a value of $-14.90$ [dm g/cm$^3$]$^{-1}$ was reported in [19].

The availability of an experimental gas phase specific rotation at 355 nm of *S*-propylene oxide seems to have reinforced the interest in this system. Thus, Giorgio et al. [15] were able to reproduce the experimental order of magnitude as well as sign using DFT/B3LYP theory. Subsequently, using approximate as well as full coupled cluster singles and doubles theory and large basis sets, neither Pedersen et al. [2] nor Tam et al. [10] obtained the correct sign. As suggested by Tam et al. [10], this is most likely due to the fact that the lowest excitation energy calculated at the DFT/B3LYP level is too small, thereby forcing the ORD curve to change sign at a too large wave length. In this Letter, we elaborate on the work of the Crawford group by taking into account the effect of triples excitations in the CC treatment and eliminating the origin-dependence by using the MVG formulation. We calculate the gas phase optical rotation using the coupled cluster hierarchy CCS, CC2 [20], CCSD [21], and CC3 [22,23] of CC response functions. The effect of triples as included in the CC3 model is important for obtaining quantitative agreement with experiment. This has been demonstrated for a variety of molecular linear and non-linear optical properties. In fact, when triples are considered the accuracy often surpass the one obtained by experiment. It is therefore interesting to explore if triples can lead to an accordance between the calculated and experimental OR.

Experimentally, Kumata et al. [17] and Müller et al. [18] have observed substantial solvent effects at 589.3 and 355 nm, respectively, showing that theoretical modeling of such effects is imperative. In this Letter, therefore, we present CC calculations of solvent effects on the optical rotation of *S*-propylene oxide and compare them to available theoretical as well as experimental results. We carry out condensed phase calculations using the CC2 and CCSD models combined with a (non-equilibrium) single center multipole based spherical cavity dielectric continuum (DC) model for the solvent. Recently, we have applied this combined coupled cluster/dielectric continuum (CC/DC) [24] model to study solvent effects on rotatory strength tensors of formaldehyde as well as to the $n \rightarrow \pi^*$ electronic transition in cyclopropanone and related natural optical active molecules (see [25]).

Due to the complete neglect of structural effects in the DC model, this description of the environment may be expected to underestimate the solvent effects (see for example the discussion in [25]). Thereby, solvent descriptions based on explicit models, for example

combined quantum mechanics and molecular mechanics (QM/MM) methods, are generally considered as superior to the DC models. However, due to the significant number of solute-solvent configurations needed in the statistical analysis of solvent effects based on the QM/MM models (and thereby a drastic CPU time requirement), we find that the DC model may be used as a preliminary study of the solvent effects on the ORD of *S*-propylene oxide.

## 2. Computational details

We have calculated the ORD of *S*-propylene oxide in gas phase and in solution using a local version of the DALTON program package [26]. Due to the rigidity of *S*-propylene oxide, conformational averaging over molecular geometries is neglected. Furthermore, in the condensed phase calculations we do not consider geometrical distortions due to the perturbation of the solvent, i.e. we use the gas phase geometry. In all the correlated property calculations the lowest orbitals of 1s character on carbon and oxygen have been frozen. The geometry of *S*-propylene oxide has been optimized at the DFT level using the B3LYP functional and the cc-pVTZ basis. Furthermore, in order to explore the effect of changes in the molecular geometry on the ORD, we have also geometry optimized *S*-propylene oxide using B3LYP/6-31G* and Møller-Plesset second order perturbation theory (MP2) combined with the cc-pVTZ basis set (MP2/cc-pVTZ). Fig. 1 shows the geometry of *S*-propylene oxide.

The basis sets used in the property calculations are the Sadlej basis set (which amounts to a total of 150 contracted Gaussian functions) and a basis set denoted A. The A basis set consists of the aug-cc-pVDZ basis set for carbon, the aug-cc-pVTZ basis set for oxygen, and the d-aug-cc-pVDZ basis set for hydrogen. It has been chosen from a basis set convergence analysis of the lower excitation energies of ethylene oxide ($C_2H_4O$), which is similar to but smaller and more symmetric ($C_{2v}$) than propylene oxide. In the largest calculations on ethylene oxide, an all-atom d-aug-cc-pVTZ basis set computation was performed (using the CCSD method), and for the four lowest excitation energies the deviations in this calculation and the one using the A basis set were at most 0.2 eV. We note that the four lowest excitations in ethylene oxide are Rydberg-like excitations, which usually imply that a double augmentation in the basis set is crucial. Furthermore, the inclusion of diffuse functions has previously been found to be important for calculating the electric dipole–magnetic dipole polarizability, see e.g. [13] (limited to the static approach for calculation of $\beta'$) and the discussion in [10]. However, as stated above, including only a double augmentation in the hydrogen basis set reproduces the all-atom d-aug-cc-pVTZ basis set calculation with sufficient accuracy, thereby leading to a medium sized basis set (193 contracted Gaussians) to be used in the property calculations. The calculations employing the Sadlej basis set have been performed, since this basis set in combination with DFT/B3LYP previously has predicted the specific rotation of *S*-propylene oxide at 355 nm successfully [15].

In the solvent calculations local field factors are assumed to be equal to unity. In these calculations the cavity radius is equal to the distance from the center-of-mass to the most distant hydrogen atom plus the van der Waals radius of hydrogen, i.e. 6.701 a.u., and the multipole expansion of the solute molecular charge distribution is truncated at a maximum of $L_{max} = 10$ if not stated differently.

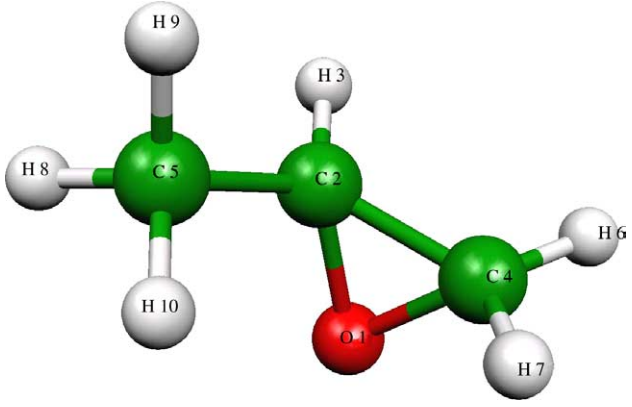



Fig. 1. Geometry and definition of atomic labels for *S*-propylene oxide.

## 3. Results and discussion

### 3.1. Gas phase results

As discussed in Section 1, the central molecular quantity in connection with ORD is the electric dipole–magnetic dipole polarizability. It is well known that this response function has (first order) poles at the position of the electronic excitation energies, and that the corresponding residues are directly related to the isotropic rotatory strengths. Furthermore, the polarizability is often dominated by the contributions due to the lowest electronic transitions, a point which has been utilized in the so-called few-states models. Correspondingly, an accurate prediction of the polarizability, and thereby the ORD, usually requires an elaborate pole structure of the electric dipole–magnetic dipole polarizability.

In Table 1, we have shown the four lowest electronic excitation energies together with the corresponding oscillator and rotatory strengths. Experimentally, the lowest excitation ($n_O \rightarrow 3s$) is found to be located in the region of 174.2–175.4 nm (7.12–7.07 eV) in the gas

Table 1
The four lowest electronic excitation energies, $E_{ex}$ (eV), of propylene oxide

| Basis set | Model | $E_{ex}$ | ${}^nf_r$ | ${}^nf_v$ | ${}^nR_r$ | ${}^nR_v$ |
|---|---|---|---|---|---|---|
| Sadlej | CC2 | 6.38 | 0.016 | 0.015 | 18.24 | 17.76 |
| | | 6.81 | 0.008 | 0.008 | −6.63 | −6.20 |
| | | 6.88 | 0.020 | 0.020 | −0.31 | −0.05 |
| | | 7.02 | 0.023 | 0.022 | −5.42 | −5.26 |
| | CCSD | 7.14 | 0.012 | 0.011 | 17.41 | 17.32 |
| | | 7.43 | 0.016 | 0.019 | 5.22 | 5.98 |
| | | 7.59 | 0.017 | 0.017 | −9.48 | −9.48 |
| | | 7.80 | 0.022 | 0.022 | −7.38 | −7.49 |
| | CC3 | 7.17 | 0.014 | 0.013 | 20.15 | 19.78 |
| | | 7.47 | 0.013 | 0.014 | 3.54 | 4.04 |
| | | 7.64 | 0.018 | 0.017 | −9.63 | −9.49 |
| | | 7.82 | 0.024 | 0.024 | −8.75 | −8.71 |
| A | CC2 | 6.52 | 0.015 | 0.014 | 16.54 | 15.95 |
| | | 6.92 | 0.006 | 0.006 | 0.18 | 0.64 |
| | | 6.97 | 0.019 | 0.019 | −5.70 | −5.58 |
| | | 7.13 | 0.019 | 0.018 | −4.82 | −4.65 |
| | CCSD | 7.31 | 0.011 | 0.010 | 16.39 | 16.17 |
| | | 7.55 | 0.015 | 0.018 | 5.20 | 5.86 |
| | | 7.75 | 0.015 | 0.015 | −8.47 | −8.39 |
| | | 7.95 | 0.019 | 0.020 | −6.76 | −6.85 |
| Experimental [27] $n_O \rightarrow 3s$ | | 7.12 | 0.025 | | 11.8 | |
| Experimental [27] $n_O \rightarrow 3p$ | | 7.75 ($\overline{E}_{ex}$) | 0.062 ($\sum^n f$) | | −10.8 ($\sum^n R$) | |
| Experimental [28] $n_O \rightarrow 3s$ | | 7.07 | – | | 12.56 | |
| Experimental [28] $n_O \rightarrow 3p$ | | 7.70 ($\overline{E}_{ex}$) | – | | −6.98 ($\sum^n R$) | |

Also given are the dimensionless oscillator strength (using length and velocity gauges, ${}^nf_r$ and ${}^nf_v$), and the rotatory strength (in $10^{-40}$ cgs, using length and velocity gauges, ${}^nR_r$ and ${}^nR_v$). The origin is in the center of mass and the structure used is B3LYP/cc-pVTZ. The symbol $\overline{E}_{ex}$ is the mean excitation energy while the symbol $\sum^n f$ ($\sum^n R$) represents the total oscillator (rotatory) strength of the three $n_O \rightarrow 3p$ excitations.

phase absorption spectrum [27,28]. For this excitation, an oscillator strength of 0.025 and rotatory strengths around 11.8–$12.56 \times 10^{-40}$ cgs have been reported [27,28]. As seen from Table 1, the theoretical predictions of the oscillator strengths are thus too small and the rotatory strengths are slightly overestimated compared to experimental data. The deviations between the length and velocity gauges are rather small, and deviations, as compared to experimental data, are probably due to basis set and electron correlation effects. Concerning the theoretical prediction of the lowest electronic excitation energy, we find that the CCSD method compares excellently with experimental data, while the CC2 model underestimates the electronic excitation energy by 0.6–0.7 eV. Experimentally, the three $n_O \rightarrow 3p$ excitations are found around 160–161.1 nm (7.70–7.75 eV) in the gas phase absorption spectrum and the corresponding (total) oscillator strength is approximately 0.062, while the rotatory strength has been reported to be around $-6.98$ to $-10.8 \times 10^{-40}$ cgs [27,28]. From the results in Table 1, we find a relatively good prediction using CCSD (a mean excitation of 7.61 eV for the Sadlej basis set and 7.75 for the A basis set) while, again, the CC2 results are underestimated as compared to experiment. As with the first excitation, the deviations between the length and velocity gauges are minor, and in all cases a (total) negative rotatory strength is predicted for the three $n_O \rightarrow 3p$ excitations. The magnitude of the total rotatory strength is in the intervals from $-9.38$ to $-11.6 \times 10^{-40}$ cgs for CCSD and $-9.59$ to $-12.43 \times 10^{-40}$ cgs for CC2 using either basis set. From the results in Table 1 we hence conclude that the CCSD results for the four lowest electronic excitations together with the oscillator and rotatory strengths compare fairly well with experimental data. In addition, the electronic excitation energies compare well with the CCSD results of [10] and the DFT results of [29] using the SAOP Kohn–Sham potential. Comparing the experimental results and the B3LYP/Sadlej results of [15] ($E_{ex} = 6.56$, $R_r = 20 \times 10^{-40}$ cgs, and a group excitations at 7.05–7.43 eV with a total rotatory strength of $-27 \times 10^{-40}$ cgs) with our CCSD predictions, we find that the CCSD results are superior. In addition to the presented CC2 and CCSD results in Table 1, we have also used the CC3 model to estimate the effects of including triples excitations. While all CC3 results for the Sadlej basis set are computed, we only calculate the excitation energies with the A basis set ($E_{ex} = 7.27, 7.53, 7.73, 7.91$ eV). Hence, the triples effects on the excitation energies are found to be small ($\lesssim 0.6\%$), thus supporting the high accuracy of the CCSD results. With the Sadlej basis set, Table 1 shows that the triples effects on the oscillator and rotatory strengths are modest, and the sum of the four lowest rotatory strengths is decreased by approximately 10% going from CCSD to CC3 in either gauge formulations.

Turning now to the gas phase OR, Table 2 reports the CCS, CC2, CCSD, and CC3 specific rotation as well as the origin-dependence for *S*-propylene oxide using the B3LYP/cc-pVTZ structure. The coordinate system to which the origin-dependence vector refers is identical to that of [2]. For the LG results we use the center of mass as origin. The origin-dependence of the LG specific rotation is significant for both basis sets, even with the CC3 model, and increases as the wave length decreases. In fact, at 355 nm, the CC2 LG specific rotation would be positive using the Sadlej basis with the origin located at C4 (see Fig. 1). Note that the components of $\mathbf{\Delta}$ vary non-smoothly with respect to both the basis set and the level of electron correlation. In the present case, the overall origin-dependence follows the pattern $\mathrm{CCS} \gg \mathrm{CC2} \approx \mathrm{CCSD} > \mathrm{CC3}$ in accordance with the fact that the correlation description is improved and the origin-dependence vanishes in a full correlation treatment using a complete basis set. We also note that the CC2/A results in this work compare well with the CC2/d-aug-cc-pVQZ results reported in [2] using Cholesky decomposition-based CC2 linear response theory [3], and exactly the same structure of *S*-propylene oxide as in this work. This clearly indicates the high flexibility of the A basis set used in this study. Also, we find that the origin-dependence at the CCSD level is of the same magnitude as reported by Tam et al. [10]. The effect of coupled cluster triples excitations is a decrease of the magnitude of the LG specific rotation as compared to the CCSD results. On the other hand, a quite large increase is observed for the MVG results going from CCSD to CC3 with the Sadlej basis set at 355 nm. Using both the LG as well as the origin invariant MVG formulation, all models beyond the Hartree–Fock-like CCS method predict a sizable negative specific rotation at 355 nm in contrast to the experimental result of Müller et al. [18] and the DFT/B3LYP results of Giorgio et al. [15] and Tam et al. [10]. Since self-consistent-field (SCF) calculation predicts the specific rotation to be −14.4 deg [dm g/cm$^3$]$^{-1}$ (LG at the center of mass and using the A basis set), it is noteworthy that electron correlation as described by CC theory tends to *increase* the disagreement with experiment.

In addition to the results presented in Table 2, we have also performed calculations of the OR using CCSD combined with either the A or Sadlej basis sets including additional diffuse functions placed at the center-of-mass (CM). The diffuse CM basis functions were added systematically using sets of s, p, d and potentially f primitive functions, e.g. CM2 (2s2p2d), CM2f (2s2p2d2f), CM3 (3s3p3d) and CM3f (3s3p3d3f). The exponents were chosen in an even-tempered way using 0.0100, 0.0033 for the CM2 (f) sets and 0.0100, 0.0033, 0.0011 for the CM3 (f) sets [30]. However, the specific rotations calculated using these extended basis sets deviated only slightly from the results presented in Table 2. Also, the four lowest excitation energies and the corresponding oscillator/rotatory strengths were effectively unchanged upon including the extra sets of diffuse functions. Thereby, we conclude that the A basis set possesses the flexibility to describe the excited Rydberg states of *S*-propylene oxide.

The CC results presented here do not include the effect of zero point vibration. Using SCF theory, the zero point vibrational effect has been estimated by Ruud et al. [31] to be 3.62 deg [dm g/cm$^3$]$^{-1}$ at 589.3 nm, seemingly too small to account for the different signs of the experimental and theoretical results at 355 nm.

Table 2
The MVG and LG specific rotation (deg [dm g/cm$^3$]$^{-1}$) of *S*-propylene oxide calculated at different wave lengths (nm) and the LG origin-dependence vector (deg [dm g/cm$^3$]$^{-1}$ bohr$^{-1}$)

| Wave length | Basis set | Model | $[\alpha]_{\bar{\nu}}$ | | $\mathbf{\Delta}$ | | |
|---|---|---|---|---|---|---|---|
| | | | MVG | LG | $x$ | $y$ | $z$ |
| 355 | Sadlej | CCS | 33.7 | −8.9 | 9.1 | 98.0 | 43.6 |
| | | CC2 | −18.4 | −1.6 | −9.0 | 11.4 | −0.7 |
| | | CCSD | −11.3 | −18.2 | −2.4 | 21.3 | 0.0 |
| | | CC3 | −24.0 | −17.0 | −2.3 | −0.6 | −6.1 |
| | A | CCS | 22.0 | −5.3 | −70.1 | 13.7 | −80.2 |
| | | CC2 | −56.2 | −24.7 | −5.5 | 6.3 | −1.0 |
| | | CCSD | −35.1 | −29.9 | −10.7 | 2.2 | −12.6 |
| | | CC3 | – | −23.2 | 6.0 | 4.1 | 3.7 |
| 589.3 | Sadlej | CCS | 5.7 | −7.3 | 2.8 | 32.9 | 14.8 |
| | | CC2 | −26.8 | −21.6 | −2.3 | 3.3 | −0.1 |
| | | CCSD | −15.0 | −16.5 | −0.8 | 7.0 | 0.1 |
| | A | CCS | 1.7 | −6.3 | −23.7 | 4.7 | −26.7 |
| | | CC2 | −35.1 | −25.9 | −1.3 | 2.4 | −0.5 |
| | | CCSD | −21.2 | −19.2 | −3.5 | 0.8 | −4.1 |
| | | CC3 | – | −17.7 | 2.0 | 1.4 | 1.3 |

The origin is in the center of mass and the structure used is B3LYP/cc-pVTZ.

However, further investigations where the zero point vibrational effect is considered at a correlated level of theory are clearly desirable.

In this Letter, we shall limit ourselves to an investigation of the dependence of the specific rotation on the molecular structure. Fig. 2 depicts the CC2/A and CCSD/A LG ORD curves for *S*-propylene oxide for three different geometries optimized at the MP2/cc-pVTZ, B3LYP/6-31G*, and B3LYP/cc-pVTZ levels. In all cases, the origin is in the center of mass. The molecular structures only deviate negligibly from each other, the largest difference being in the $C_2C_5$ bond distance (0.011 Å) and in the $H_6C_4H_7$ angle (1.1°), and all structures compare well with experimental data [32]. As seen from Fig. 2, the ORD curves for different geometries deviate most as the wavelength is decreased, and around 355 nm the CC2 results deviate ~7 deg [dm g/cm$^3$]$^{-1}$. For comparison, the corresponding deviations at 589.3 nm are ~2.5 deg [dm g/cm$^3$]$^{-1}$. Thus, as previously observed in [10], the geometry has a significant effect on the computed specific rotations. Thereby, vibrational effects may be crucial.

Summarizing, we state that in light of the high quality of the coupled cluster results, it is difficult to perceive how an agreement in sign can be obtained between the experimental and wave function based calculated OR without considering vibrational contributions. This should particular be seen in the light of the large shift in the OR with only small perturbations in the molecular geometry (Fig. 2). Thus, the effect of zero point vibrational contribution at 355 nm and at a correlated level of theory is desirable.

### 3.2. Condensed phase results

Turning now to the question of solvent effects, we note that these have traditionally been included by calculating local field factors based on the Lorentz approach [33]. However, as seen in for example [6], inclusion of these field factors may lead to results which are actually further away from the experimental condensed phase results than the vacuum values. Consequently, solvent effects require special attention.

In Table 3, we report the LG specific rotation for *S*-propylene oxide (B3LYP/cc-pVTZ structure) calculated at 355 nm using CC2 combined with the A basis set for different orders of truncation of the multipole expansion. The solvent is $CH_3CN$. From this table, we first observe that including only the $l = 1$ term, which is equivalent to the Onsager solvation model [33], leads to a significant solvent effect. However, going beyond this approach reduces the solvation effect and a rather slow convergence is observed, leading to the conclusion that $L_{max} \simeq 9$–10 should be used in order to obtain converged results. The conclusion concerning the rather large magnitude of $L_{max}$ when modeling magnetic properties has also been observed in for example [34]. Second, we observe that the effect of the solvent is to

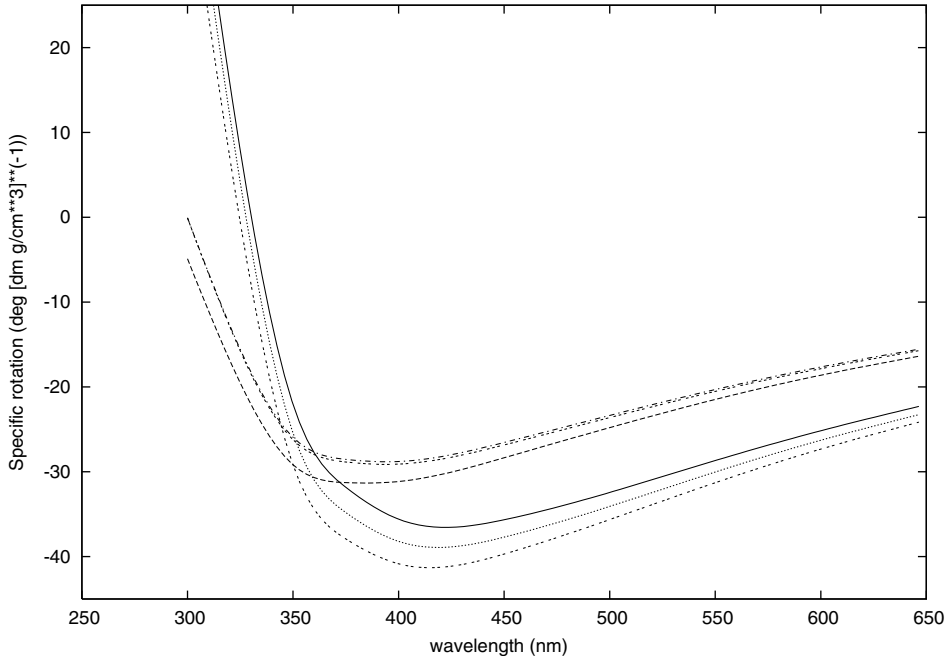



Fig. 2. LG optical rotatory dispersion (deg [dm g/cm$^3$]$^{-1}$) curves of *S*-propylene oxide calculated using CC2/A and CCSD/A and different molecular structures. The origin is in the center of mass. The results for CCSD(MP2/cc-pVTZ) and CCSD(B3LYP/6-31G*) nearly falls on the same curve. (——): CC2 (B3LYP/cc-pVTZ); (------): CCSD (B3LYP/cc-pVTZ).; (·····): CC2 (MP2/cc-pVTZ) (·–·–·–): CCSD (MP2/cc-pVTZ); (-- --): CC2 (B3LYP/6-31G*); (--- ---): CCSD (B3LYP/6-31G*).

Table 3
The LG specific rotations (deg [dm g/cm$^3$]$^{-1}$) of *S*-propylene oxide calculated at 355 nm using CC2 with the A basis set and different orders of the multipole expansion ($L_{max}$)

| $L_{max}$ | 0 | 1 | 2 | 3 | 4 | 5 | 6 | 7 | 8 | 9 | 10 |
|---|---|---|---|---|---|---|---|---|---|---|---|
| [α] (355 nm) | −24.7 | −48.8 | −33.5 | −34.6 | −34.2 | −33.7 | −34.2 | −33.3 | −32.9 | −32.7 | −32.7 |

The solvent is $CH_3CN$ ($\epsilon_{st}$ = 36.64 and $\epsilon_{op}$ = 1.806). The origin is in the center of mass and the structure used is B3LYP/cc-pVTZ.

enhance the magnitude of the specific rotation. For *S*-propylene oxide in $CH_3CN$, the solvent effect is thus −8 deg [dm g/cm$^3$]$^{-1}$.

Table 4 gives the LG specific rotation for *S*-propylene oxide calculated at 355 nm and at 589.3 nm using CC2 and CCSD in vacuum and in seven representative solvents ordered according to polarity. The results are computed with the A basis set. In addition, we have included condensed phase results obtained by employing the Lorentz local field factors. We note that solvent effects based on the Lorentz model may be attributed to two effects: (i) the cavity-field and (ii) the reaction field. Thereby, the derived quantities are termed effective properties. In contrast, the DC model provides solute properties (including only the effect of the reaction field) and the two kinds of properties (effective and solute) are thereby not directly comparable. Finally, we tabulate the results computed by Mennucci et al. [14] using the DFT dynamical approach implemented in combination with the polarizable continuum model (PCM) [35], and report the available experimental data. From Table 4, we first observe that for the ab initio CC2 and CCSD results, respectively, the results for the specific rotation are very similar for the apolar solvents. Likewise, the specific rotation give almost identical results in the two high dielectric constant (polar) solvents. This trend has also been observed in [14]. Going from vacuum to the first solvent leads to an increase in the magnitude of the specific rotation. Passing to the solvents $CCl_4$ and $C_6H_6$ the magnitude of the specific rotation is increased further. Note that benzene is the solvent with the largest optical dielectric constant. Continuing to the more polar solvent $CHCl_3$, the magnitude of the specific rotation decreases and this decrease continues as the solvents become more polar. In the apolar solvents, the effect of the environment is more significant at 355 nm than at 589.3 nm and, in general, the effect is rather small for the polar solvents. The Lorentz corrected results are seen to overestimate the effect of solvation as compared to available experimental data. Also, in the very polar solvents, the Lorentz model may lead to results for the specific rotation which exhibit solvent effects in qualitative disagreement with the CC/DC description as compared to the specific rotation of *S*-propylene in vacuum, e.g. for the polar solvents the Lorentz model predicts an increase in the magnitude of the specific rotation whereas the CC/DC model predicts a decrease.

Considering the different solvent models it is worth noting that, even though most of the signs of the calculated OR's are in accord with the experimental data, neither of them is capable of reproducing the relative experimental shifts when the solvent change. Specially, the solvent models are not capable of reproducing the experimentally established sign change in the 589.3 nm OR in the case of an aqueous solution. All models predicts an almost monotonical behavior of the specific rotation as a function of the solvent polarity. Further for the DC and PCM models, the vacuum contribution dominate, and the solvent contribution represents only a small perturbation. In contrast, we have in the experimental results (at 355 nm) a sign change in the OR going from vacuum to the condensed phase. Agreement in sign between the DC solvent model and experiment can thus not be used to justify the reliability of the solvent model.

Table 4
The LG specific rotation (deg [dm g/cm$^3$]$^{-1}$) of *S*-propylene oxide calculated at different wave lengths (nm) and for different solvents

| [α] | Vacuum | $C_6H_{12}$ | $CCl_4$ | $C_6H_6$ | $CHCl_3$ | $(CH_3)_2CO$ | $CH_3OH$ | $H_2O$ |
|---|---|---|---|---|---|---|---|---|
| CC2 (355 nm) | −24.7 | −38.0 | −38.7 | −39.6 | −37.1 | −33.3 | −32.2 | −32.1 |
| CC2 (589.3 nm) | −25.9 | −30.1 | −30.2 | −30.6 | −29.0 | −27.2 | −26.7 | −26.7 |
| CCSD (355 nm) | −29.9 | −37.5 | −37.6 | −38.4 | −33.7 | −28.7 | −27.6 | −27.3 |
| CCSD (589.3 nm) | −19.2 | −22.0 | −22.0 | −22.3 | −20.6 | −18.8 | −18.5 | −18.4 |
| Lorentz corrected CCSD (355 nm) | – | −40.1 | −41.2 | −42.3 | −40.7 | −38.3 | −37.5 | −37.7 |
| Lorentz corrected CCSD (589.3 nm) | – | −25.8 | −26.4 | −27.2 | −26.1 | −24.6 | −24.1 | −24.2 |
| Experimental (355 nm) [18] | 10.2 ± 2.9 | −26.4 | – | – | – | – | – | – |
| Experimental (589.3 nm) [17] | – | −11.9 | −18.7 | −30.6 | −8.5 | −8.2 | −7.2 | +4.3 |
| B3LYP/aug-cc-pVDZ PCM (589.3 nm) [14] | −17.5 | −14.7 | −14.2 | −14.1 | −11.6 | −9.2 | −8.9 | – |

The basis set used is the A basis set. The origin is in the center of mass and the structure used is B3LYP/cc-pVTZ. The dielectric constants are $C_6H_{12}$: $\epsilon_{st}$ = 2.028 and $\epsilon_{op}$ = 2.028; $CCl_4$: $\epsilon_{st}$ = 2.228 and $\epsilon_{op}$ = 2.129; $C_6H_6$: $\epsilon_{st}$ = 2.247 and $\epsilon_{op}$ = 2.244; $CHCl_3$: $\epsilon_{st}$ = 4.900 and $\epsilon_{op}$ = 2.085; $(CH_3)_2CO$: $\epsilon_{st}$ = 20.70 and $\epsilon_{op}$ = 1.841; $CH_3OH$: $\epsilon_{st}$ = 32.63 and $\epsilon_{op}$ = 1.758. $H_2O$: $\epsilon_{st}$ = 78.54 and $\epsilon_{op}$ = 1.778.

## 4. Concluding remarks

In this Letter, we have presented calculations of the optical rotatory dispersion of *S*-propylene oxide in both gas and condensed phases. The electronic structure method used is the coupled cluster hierarchy including the highly correlated CC3 method. In contrast to the experimentally established positive sign of the specific rotation of *S*-propylene oxide in gas phase at 355 nm, all methods (beyond CCS) used in this Letter yield negative values for the specific rotation (using the center of mass as origin for the LG results). At the same time, the predicted results for the lowest electronic excitation energies and the corresponding (isotropic) rotatory strengths are in line with the experimental results. Considering the high quality of the CC3 model makes it difficult to perceive how an agreement can be obtained between the signs of the experimental and wave function based calculated OR without considering vibrational effects. A reinvestigation of the zero point vibrational contribution at 355 nm at a correlated level is therefore desirable. Concerning the condensed phase calculations, the solvent has been modeled as a dielectric continuum. The calculated solvent contributions are found to be rather small compared to the vacuum contribution. Furthermore, the solvent contributions are unable to reproduce the relative experimental shifts as the solvent changes. We attribute this to the complete neglect of structural effects in the dielectric solvent model. It is well known that a chiral solute will induce a chiral solvent structure even if the individual solvent molecules are achiral. This means that one part of the observed ORD is due to the chiral solvent shell, and another part originates from the chiral solute molecule. In the DC description, the solvent is treated as a homogeneous medium, and the contribution from the solvent shell to the ORD is not accounted for. Thereby, calculations using more elaborate solvent models where structural effects are considered in detail would be desirable to shed some light on the controversy between the calculated and experimental observed OR for *S*-propylene oxide.

## Acknowledgements

P.J. acknowledges support by Statens Naturvidenskabelige Forskningsråd (SNF) and Danish Center for Scientific Computing (DCSC). K.V.M. thanks SNF, Statens Teknisk Videnskabelige Forskningsråd (STVF), DCSC, and the EU networks NANOQUANT, MOLPROP and THEONET II for support. T.B.P. acknowledges support from THEONET II. F.P. acknowledges support from Carlsbergfondet.

## References

[1] T.B. Pedersen, B. Fernández, H. Koch, J. Chem. Phys. 114 (2001) 6983.
[2] T.B. Pedersen, H. Koch, L. Boman, A.M.J. Sánchez de Merás, Chem. Phys. Lett. 393 (2004) 319.
[3] T.B. Pedersen, A.M.J. Sánchez de Merás, H. Koch, J. Chem. Phys. 120 (2004) 8887.
[4] R.D. Amos, Chem. Phys. Lett. 87 (1982) 23.
[5] R.K. Kondru, P. Wipf, D.N. Beratan, J. Phys. Chem. A 103 (1999) 6603.
[6] P.J. Stephens, F.J. Devlin, J.R. Cheeseman, M.J. Frisch, J. Phys. Chem. A 105 (2001) 5356.
[7] R.K. Kondru, P. Wipf, D.N. Beratan, Science 282 (1998) 2247.
[8] K. Ruud, P.J. Stephens, F.J. Devlin, P.R. Taylor, J.R. Cheeseman, M.J. Frisch, Chem. Phys. Lett. 373 (2003) 606.
[9] K. Ruud, T. Helgaker, Chem. Phys. Lett. 352 (2002) 533.
[10] M.C. Tam, N.J. Russ, T.D. Crawford, J. Chem. Phys. 121 (2004) 3550.
[11] J. Autschbach, S. Patchkovskii, T. Ziegler, S.J.A. van Gisbergen, E.J. Baerends, J. Chem. Phys. 117 (2002) 581.
[12] S. Grimme, Chem. Phys. Lett. 339 (2001) 380.
[13] J.R. Cheeseman, M.J. Frisch, F.J. Devlin, P.J. Stephens, J. Phys. Chem. A 104 (2000) 1039.
[14] B. Mennucci, J. Tomasi, R. Cammi, J.R. Cheeseman, M.J. Frisch, F.J. Devlin, J. Phys. Chem. A 106 (2002) 6102.
[15] E. Giorgio, C. Rosini, R.G. Viglione, R. Zanasi, Chem. Phys. Lett. 376 (2003) 452.
[16] K. Yabana, G.F. Bertsch, Phys. Rev. A 60 (1999) 1271.
[17] Y. Kumata, J. Furukawa, T. Fueno, Bull. Chem. Soc. Jpn. 43 (1970) 3920.
[18] T.M. Müller, K.B. Wiberg, P.H. Vaccaro, J. Phys. Chem. A 104 (2000) 5959.
[19] V. Schurig, B. Koppenhófer, W. Búrkle, Angew. Chem. 90 (1978) 993.
[20] O. Christiansen, H. Koch, P. Jørgensen, Chem. Phys. Lett. 243 (1995) 409.
[21] G.D. Purvis, R.J. Bartlett, J. Chem. Phys. 76 (1982) 1910.
[22] O. Christiansen, H. Koch, P. Jørgensen, J. Chem. Phys. 103 (1995) 7429.
[23] K. Hald, F. Pawlowski, P. Jørgensen, C. Hättig, J. Chem. Phys. 118 (2003) 1292.
[24] O. Christiansen, K.V. Mikkelsen, J. Chem. Phys. 110 (1999) 8348.
[25] J. Kongsted, Aa.E. Hansen, T.B. Pedersen, A. Osted, K.V. Mikkelsen, O. Christiansen, Chem. Phys. Lett. 391 (2004) 259.
[26] T. Helgaker et al., DALTON: a molecular electronic structure program, Release 1.2. Available from: <http://www.kjemi.uio.no/software/dalton/dalton.html>, 2001.
[27] D. Cohen, M. Levi, H. Basch, A. Gedanken, J. Am. Chem. Soc. 105 (1983) 1738.
[28] M. Carnell, S.D. Peyerimhoff, A. Breest, K.H. Gödderz, P. Ochmann, J. Hormes, Chem. Phys. Lett. 180 (1991) 477.
[29] J. Autschbach, T. Ziegler, S.J.A. van Gisbergen, E.J. Baerends, J. Chem. Phys. 116 (2002) 6930.
[30] O. Christiansen, H. Koch, P. Jørgensen, T. Helgaker, Chem. Phys. Lett. 263 (1996) 530.
[31] K. Ruud, P.R. Taylor, P.O. Åstrand, Chem. Phys. Lett. 337 (2001) 217.
[32] K.H. Hellwege, A.M. Hellwege (Eds.), Structure Data of Free Polyatomic Molecules, Landolt–Bornstein: Group II: Atomic and Molecular Physics, vol. 7, Springer, Berlin, 1976.
[33] C. Böttcher, Theory of Electric Polarization, second ed., Elsevier, Amsterdam, 1973.
[34] P.O. Åstrand, K.V. Mikkelsen, K. Ruud, T. Helgaker, J. Phys. Chem. 100 (1996) 19771.
[35] S. Miertus, E. Scrocco, J. Tomasi, Chem. Phys. 55 (1981) 117.